Tetrahedron 64 (2008) 5672–5679

Contents lists available at ScienceDirect

Tetrahedron

journal homepage: www.elsevier.com/locate/tet

Sigmatropic shifts and cycloadditions on neutral, cationic, and anionic pentadienyl+butadiene potential energy surfaces

Dustin H. Nouri, Dean J. Tantillo *

University of California, Davis, One Shields Ave, Davis, CA 95616, USA

ARTICLE INFO

Article history:
Received 18 March 2008
Received in revised form 7 April 2008
Accepted 8 April 2008
Available online 11 April 2008

ABSTRACT

Quantum chemical calculations were used to characterize [4,5] sigmatropic shifts in systems containing butadiene and pentadienyl substructures. Cationic, anionic, and radical systems with various tethers connecting these substructures were examined. In many cases, concerted [4,5] sigmatropic shifts with asynchronous bond making and breaking events were observed. The fundamental connections between [4,5] sigmatropic shifts and (5+4) cycloadditions are highlighted.

1. Introduction

The synthesis of compounds containing concatenated cyclobutane rings (ladderanes) has long stood as a daunting synthetic challenge.[1,2] Surprisingly, it has been shown that certain bacteria can produce lipids with three or five concatenated cyclobutane rings—the so-called ladderane lipids (structure **1** is an example of one type of naturally occurring [5]-ladderane lipid)[1,3]—but the biosynthetic processes that lead to these highly strained systems have not yet been characterized.

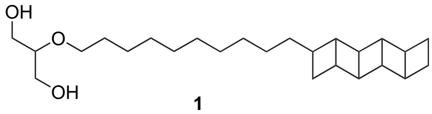

1

We have been using quantum chemical computations to probe mechanisms for ladderane formation.[1,4,5] While examining one possible pathway to [5]-ladderanes, we discovered a transformation that appears to involve a cationic [4,5] sigmatropic shift (Fig. 1).[5] This reaction involves eight rearranging electrons and the Woodward–Hoffmann orbital symmetry rules[6] would therefore predict that, under thermal conditions, this rearrangement will only be allowed for a suprafacial/antarafacial geometry. Nonetheless, the cationic sigmatropic shift shown in Figure 1 is concerted, but involves a transition state structure with a suprafacial/suprafacial geometry. At first, this appears to be a violation of the orbital symmetry rules. However, the bond breaking and making events involved in this process occur quite asynchronously.[7] The breaking σ C–C bond is only 1.60 Å long in the transition state structure while the forming σ bond is 2.18 Å long, a reasonable distance for a forming σ C–C bond.[8] Figure 2 shows the results of an intrinsic reaction coordinate (IRC, see Section 2) calculation from the transition state structure toward the product shown in Figure 1. The first structure shown as we travel from the transition state structure toward the product has a newly forming bond length of 1.69 Å, much shorter than the 2.18 Å distance in the transition state structure, while the breaking C–C bond, which was 1.60 Å long in the transition state structure, has only elongated to 1.64 Å. Clearly, bond formation largely precedes bond breaking. The Woodward–Hoffmann rules were intended to be applied to systems with cyclically delocalized transition state structures,[6] and in the reaction shown in Figure 2, the *cyclic* delocalization appears, at all points along the reaction coordinate, to be minimal at best. We therefore do not consider this reaction to be in violation of the orbital symmetry rules.

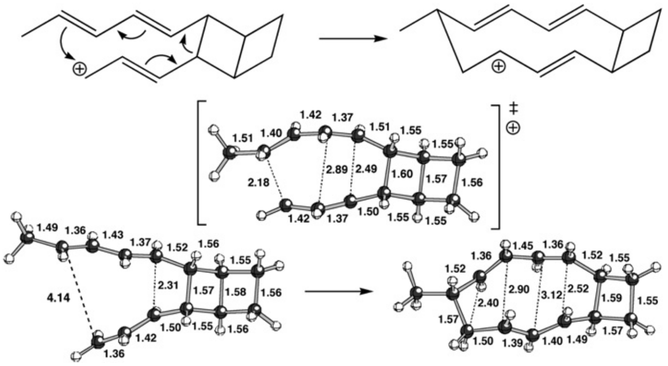

Figure 1. Computed (B3LYP/6-31G(d)) structures involved in an apparent cationic [4,5] sigmatropic shift. Select distances are shown in angstroms.

---

* Corresponding author. Tel.: +1 530 754 5635; fax: +1 530 752 8995.
E-mail address: tantillo@chem.ucdavis.edu (D.J. Tantillo).

0040-4020/$ – see front matter © 2008 Elsevier Ltd. All rights reserved.
doi:10.1016/j.tet.2008.04.028

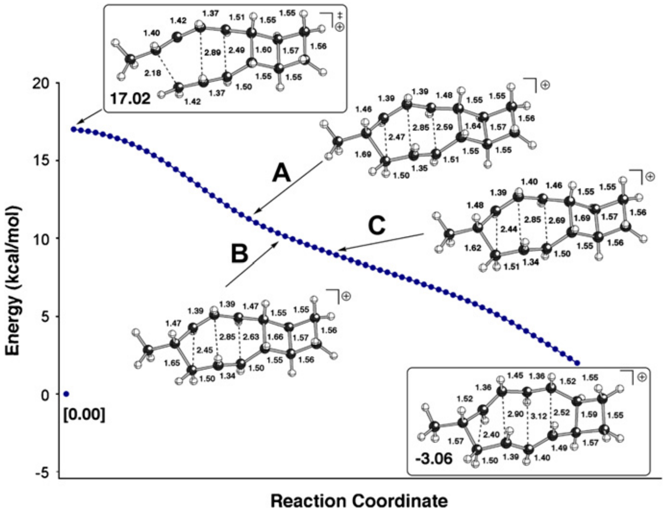

Figure 2. Intrinsic reaction coordinate (IRC) connecting the transition state structure and the product from Figure 1 (B3LYP/6-31G(d)). Structures of selected points along the IRC are shown, with selected distances in angstroms. Structures in boxes are fully optimized stationary points corresponding to the transition state structure and the minimum structure obtained from optimization of the last point of the IRC. Relative energies, without zero point energy corrections, are shown in kcal/mol.

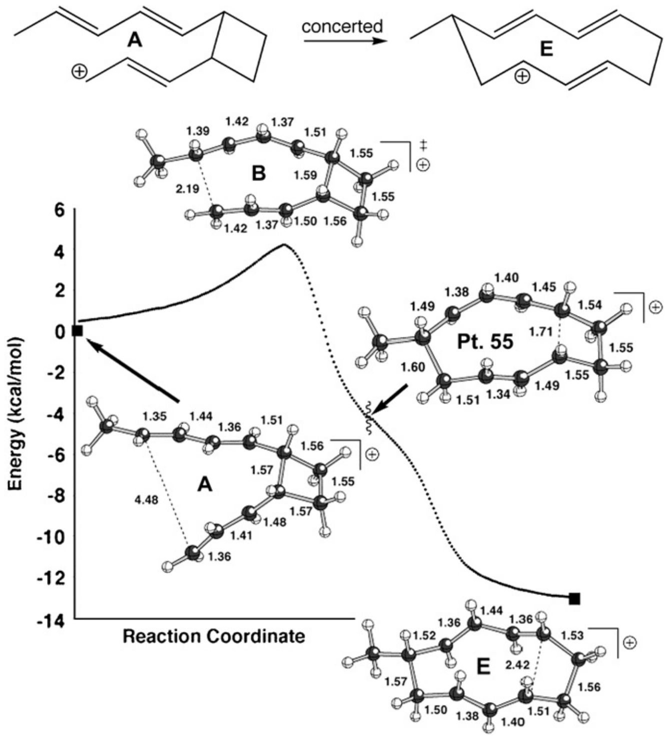

Figure 3. Computed (B3LYP/6-31G(d)) structures involved in the cationic [4,5] shift with one ethylene bridge removed. Selected distances are shown in angstroms. This IRC plot was constructed from two IRC runs: **Pt. 55** represents the last point obtained in the first IRC calculation; the IRC calculation was then continued from **Pt. 55** to intermediate **E**.

Having discovered this unusual rearrangement, we were curious as to whether concerted cationic [4,5] sigmatropic shifts would be possible for simpler systems lacking ladderane tethers. Herein, we describe how concertedness and synchronicity for this rearrangement are affected by a variety of different tethers and we examine the effects of electron count by also looking at anionic and neutral (radical) analogs.

2. Methods

All calculations were performed using the GAUSSIAN03 suite of programs.[9] Geometries were optimized at the B3LYP/6-31G(d)[10] level of theory. All stationary points were characterized by frequency analysis. Some intrinsic reaction coordinate (IRC)[11] plots were constructed from multiple IRC calculations. For each system, minima **A** and **E** were obtained by optimization of the last point located in a given IRC calculation (generally with max points=100). For cases in which multiple IRC calculations were performed to construct a single reaction path, wavy lines indicate the points where the results of two IRC calculations were joined. Structural drawings were produced using Ball & Stick.[12]

3. Structural variations

3.1. Removing rings

To see if the four-membered ring that acts as a tether for the cationic [4,5] sigmatropic shift shown in Figure 1 has a significant influence on the mechanism of this reaction, several alternative tethers were explored. First, the system was truncated to that shown in Figure 3. For this system, a concerted [4,5] sigmatropic shift was still observed, although the barrier for rearrangement is considerably less than that for the system shown above, and the exothermicity is significantly greater. It is clear from the IRC calculations that, again, C–C bond formation largely precedes C–C bond breakage. Note also that there is a shoulder on the pathway from **B** to **E**, but we were not able to locate any minimum or alternative transition state structure resembling **Pt. 55** (Fig. 3).

Next, the original system was further truncated, to form the 'parent' system, by removing another ethylene tether as well as the terminal methyl group (Fig. 4). This simple system undergoes a stepwise rather than concerted rearrangement. Note, however, that the stationary points involved in this rearrangement span an energy window of less than 8 kcal/mol. Note also the lengths of bonds a and b in the intermediate (structure **C**). The elongation of

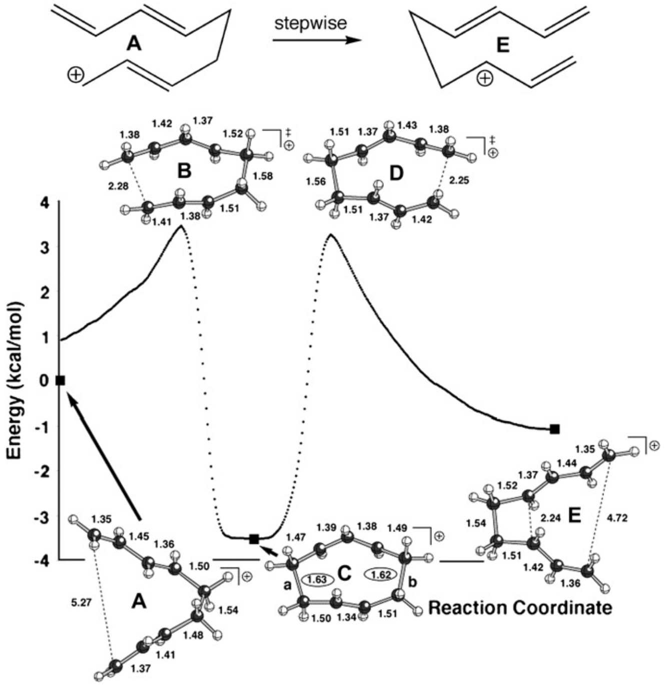

Figure 4. Computed (B3LYP/6-31G(d)) structures involved in the cationic [4,5] shift of the 'parent' system. Selected distances are shown in angstroms.

these bonds suggests that they are both interacting with the π-systems that reside between them. This can be thought of as hyperconjugation, through-bond coupling[13] of the intervening allyl and C═C π-systems, or as an indication that a pentadienyl cation+butadiene resonance structure is a significant contributor to the structure of this intermediate.[14]

3.2. Different tether lengths

Clearly, the nature of the tether influences not only the barrier and exothermicity, but also the concertedness of such rearrangements. But how is the propensity for concertedness in such shifts modulated by the strain associated with the tethers? To better address this issue, we examined systems with simple alkyl tethers of various lengths: $(CH_2)_n$ where n=4, 3, 2 (the system in Fig. 3), and 1.

When the tether length was increased to $(CH_2)_4$ (Fig. 5), we observed a stepwise pathway. Apparently, the strain in this system is low enough that the energy surface mirrors that of the unstrained parent system, with only small differences observed in terms of geometries and energetics of the species involved (compare Figs. 4 and 5).

Decreasing the length of the tether from four to three methylenes (Fig. 6) did not change the mechanism, i.e., it remained stepwise. Still, some subtle differences between this reaction and the other stepwise reactions described above were observed. First, the barrier for the second step of the rearrangement (from **C** to **E**) decreased relative to that for the case with the four-methylene tether (1.64 vs 0.53 kcal/mol). This is consistent with the three-methylene tether imparting a bit more strain on intermediate **C** than does the four-methylene tether. A slight elongation of bond b (compare Figs. 5 and 6) is also observed.

Comparing the reaction coordinates for the systems with four- (Fig. 5), three- (Fig. 6), and two-methylene (Fig. 3) tethers, we see a consistent decrease in the barrier for the second step of the rearrangement to the point where the barrier is removed completely for the two-methylene case (Fig. 7),[7] although in the two-methylene case a shoulder persists in the region of the reaction coordinate where such a barrier would be expected. This trend is consistent with the amount of strain relief expected upon the breaking of bond b for each system.

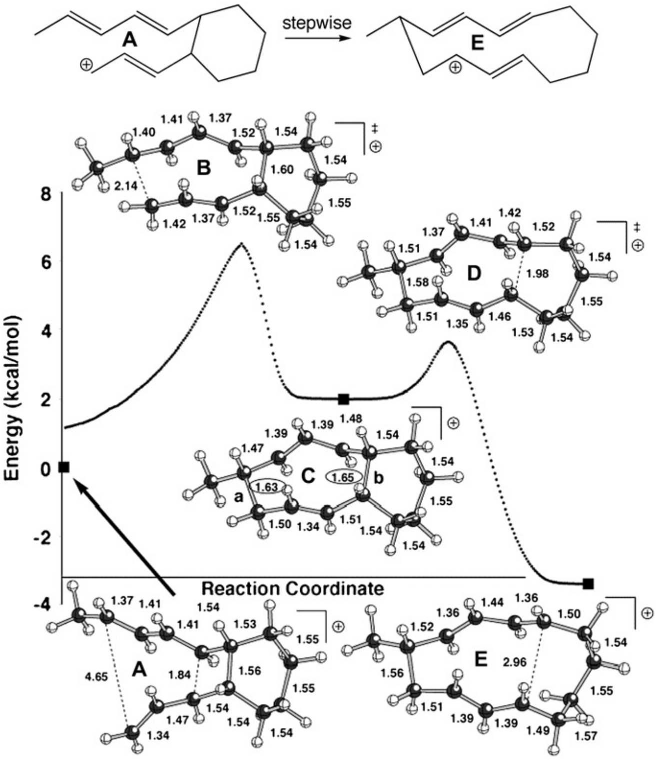

Figure 5. Computed (B3LYP/6-31G(d)) structures involved in the cationic [4,5] shift for the system with a four-methylene tether. Selected distances are shown in angstroms.

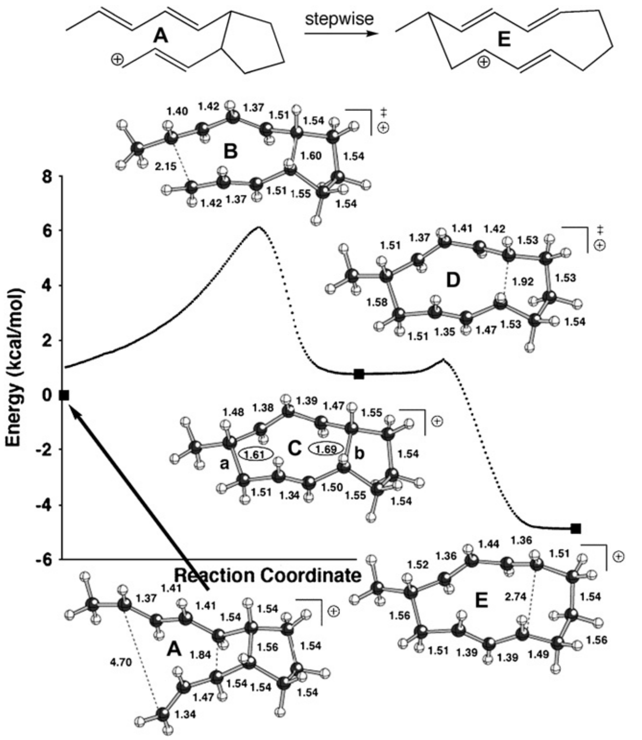

Figure 6. Computed (B3LYP/6-31G(d)) structures involved in the cationic [4,5] shift for the system with a three-methylene tether. Selected distances are shown in angstroms.

When the tether length was further reduced, down to a single methylene as shown in Figure 8, a related but different sort of reaction was observed. We were unable to locate a minimum resembling **Pt. 99** (the last structure found in the IRC calculation). Instead, structure **A′**, which does not contain the σ C–C bond expected for the **A**-type structures described above, was obtained when the geometry of **Pt. 99** was optimized. This minimum must

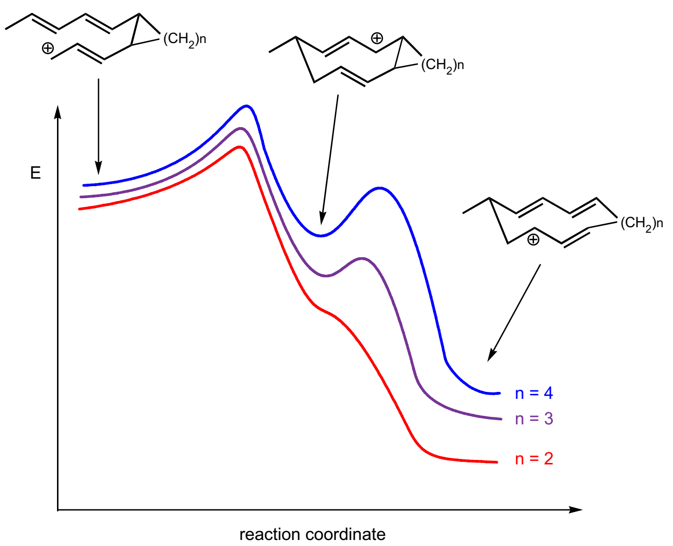

Figure 7. Qualitative reaction coordinate pictures for [4,5] sigmatropic rearrangements described above.[7]

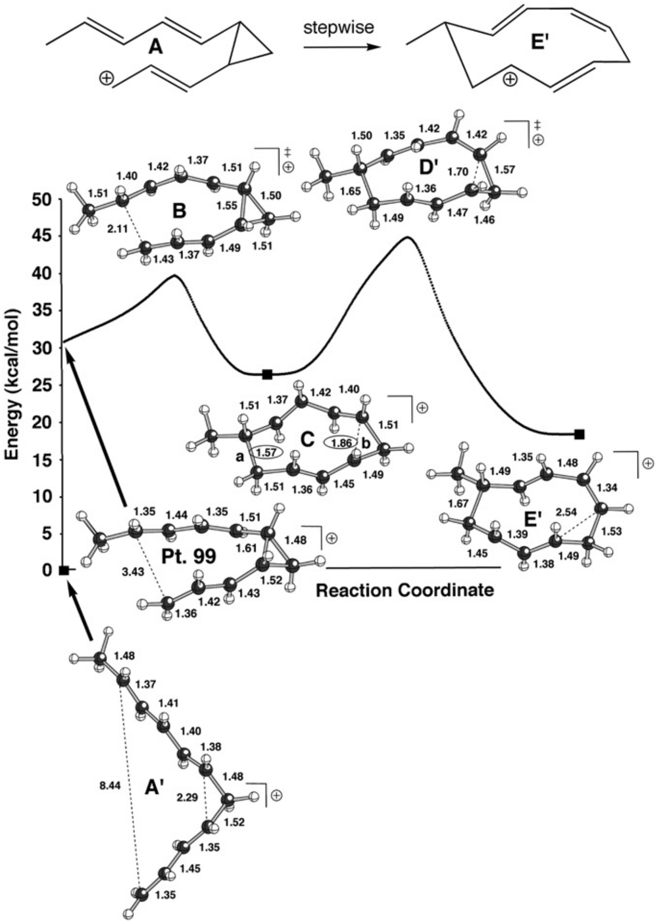

Figure 8. Computed (B3LYP/6-31G(d)) structures involved in the cationic [4,5] shift for the system with a one-methylene tether. Selected distances are shown in angstroms.

do a (5+4) cycloaddition (pentadienyl cation+butadiene) to form structure **C** (assuming that we consider the long b distance in **C** to be a bond). This sort of suprafacial/suprafacial cycloaddition is also forbidden by the Woodward–Hoffmann rules,[6] but the bond forming events that occur during this process again occur asynchronously and strong *cyclic* delocalization is again not observed at any point along the **A**′-to-**C** pathway.

Intermediate **C**, due to its long b distance, can be considered as somewhere between the **C**- and **E**-type structures described above. The elongation of distance b is likely the result of the hyperconjugation-type arguments mentioned above for the other systems, coupled with the increased strain associated with the short tether. Intermediate **C** can then be converted to a version of **E** in which one C=C unit has a *Z*, rather than *E*, geometry. The transition structure for this process, **D**′, is shown at the top right of Figure 8.

Overall, the one-methylene tether leads to a more significant change in mechanism—this system does not react via a clear-cut [4,5] sigmatropic shift nor (5+4) cycloaddition, but involves a more convoluted reaction manifold. The connections between [4,5] shifts and (5+4) cycloadditions will be described in more detail below.

3.3. Anionic analogs

Are [4,5] sigmatropic shifts still predicted to occur if two more electrons are added to the systems described above to result in anions?[15] With the addition of two electrons, each system now has a Hückel number of electrons ($4n+2=10$), and the orbital symmetry rules predict that suprafacial/suprafacial [4,5] sigmatropic shifts are now allowed. This is clear from the simple qualitative orbital pictures shown in Figure 9. The frontier orbitals involved in the anionic case have favorable interactions (Fig. 9b), while those involved in the cationic case are mismatched (Fig. 9a). Consequently, we thought that perhaps concerted and synchronous [4,5] shifts would be observed for anionic systems.

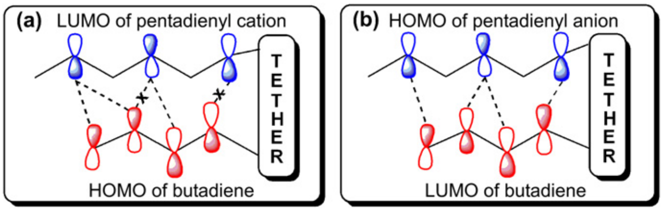

Figure 9. Frontier orbital interactions for (a) the 8 electron (cationic) and (b) the 10 electron (anionic) suprafacial/suprafacial transition structures for [4,5] sigmatropic shifts.

Figure 10 shows the parent anionic system. At first glance, the computed pathway for this system doesn't look much different from that computed for the parent cationic case. Despite the fact that a concerted rearrangement is now allowed, only the stepwise pathway was located. The intermediate on this pathway has a similar geometry to that on the cationic pathway (note that the lengths of bonds a and b for both cases are similar). The overall energetics, however, have changed significantly as the barriers for both steps have increased dramatically. It is not clear exactly why this is (it may be connected to increased electron–electron repulsion associated with the increased number of rearranging electrons), but it is interesting that in structures **A**, **B**, and **D**, the σ C–C bonds holding the two π-systems together are significantly elongated.

Different tether lengths were explored for anions as well (Figs. 11–14). Although the barriers for these systems are higher than

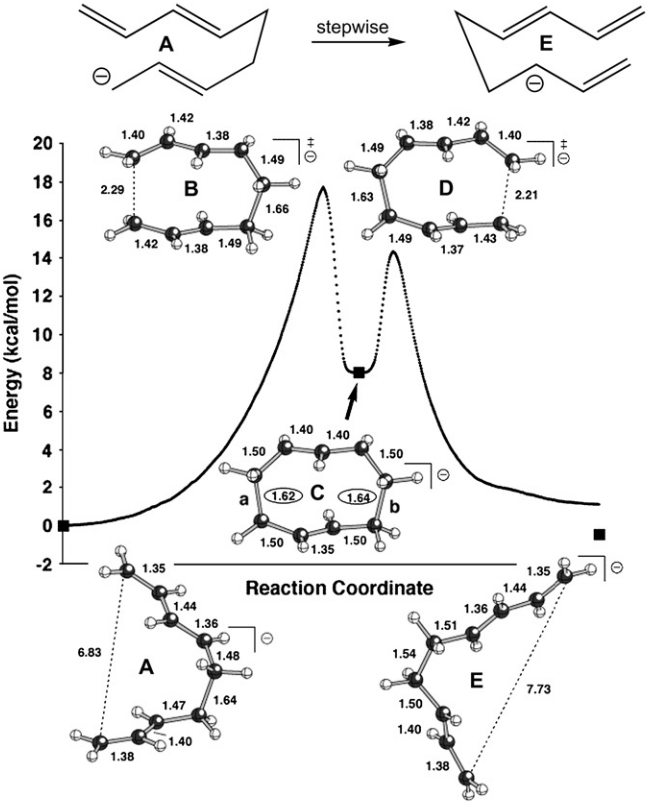

Figure 10. Computed (B3LYP/6-31G(d)) structures involved in the [4,5] shift for the parent anionic system. Selected distances are shown in angstroms.

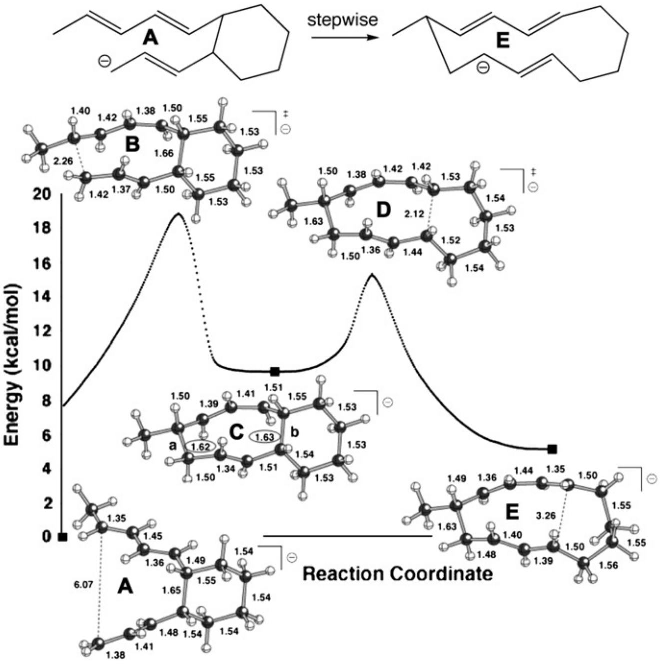

Figure 11. Computed (B3LYP/6-31G(d)) structures involved in the anionic [4,5] shift for the system with a four-methylene tether. Selected distances are shown in angstroms.

those for the cationic cases, a similar trend toward concertedness is observed. As the tether length is reduced, generally so is the barrier for the second step of the rearrangement. Unlike the cationic case, this barrier lowering is not quite enough to make any of the anionic cases truly concerted. Like the cationic case, the anionic case with a simple methylene tether again has a ring-opened reactant structure (Fig. 14, **A′**), and, unlike the cationic case, rearrangement of the anionic system with an ethylene tether also involves such a structure (Fig. 13, **A′**). Note that in these two cases, *E*/*Z* isomerization is not observed; the second step shown does correspond simply to ring opening.

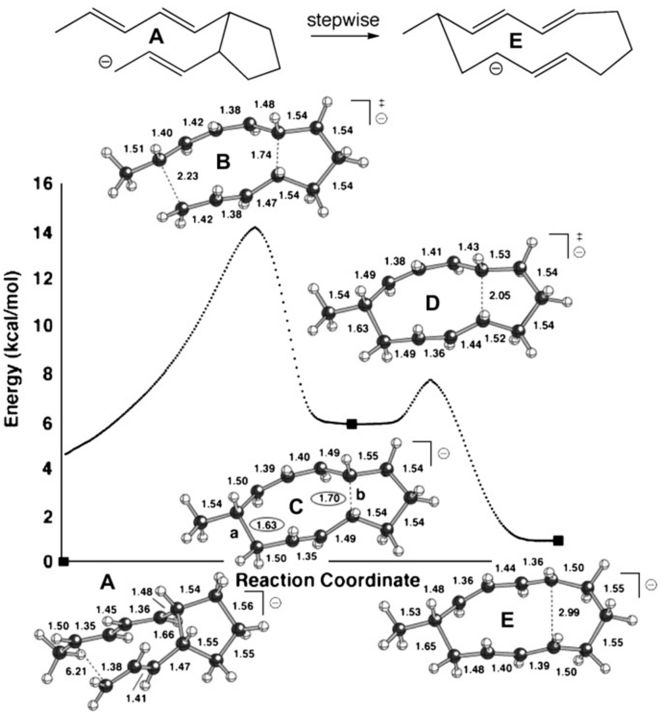

Figure 12. Computed (B3LYP/6-31G(d)) structures involved in the anionic [4,5] shift for the system with a three-methylene tether. Selected distances are shown in angstroms.

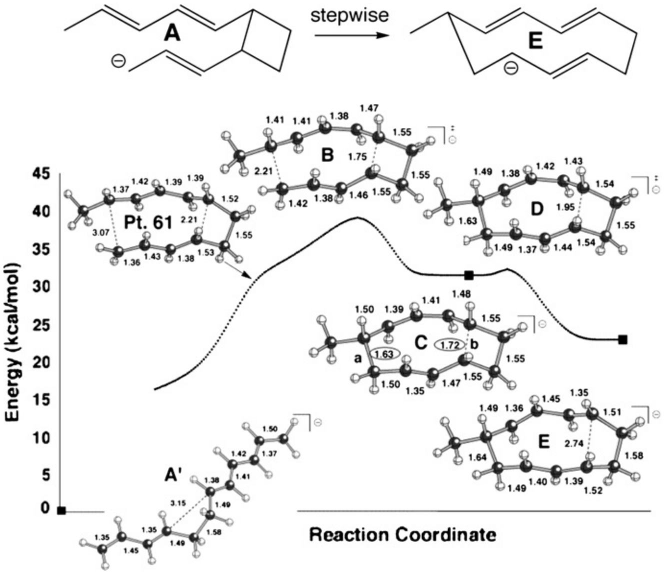

Figure 13. Computed (B3LYP/6-31G(d)) structures involved in the anionic [4,5] shift for the system with a two-methylene tether. Selected distances are shown in angstroms.

3.4. Neutral (radical) analogs

Will a [4,5] sigmatropic shift still be observed if these systems are made neutral? Such systems would have a total of nine

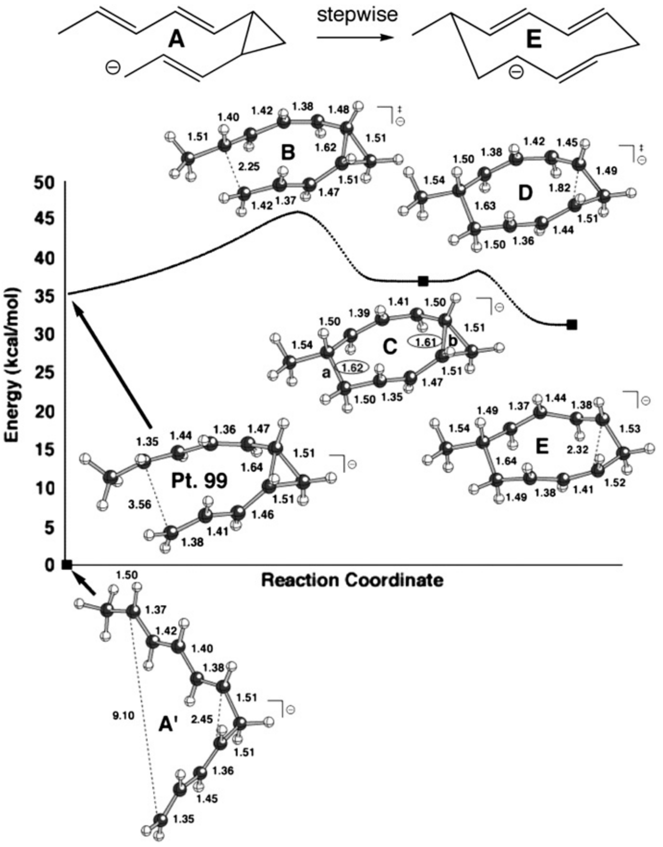

Figure 14. Computed (B3LYP/6-31G(d)) structures involved in the anionic [4,5] shift for the system with a one-methylene tether. Selected distances are shown in angstroms.

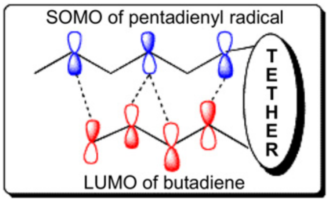

Figure 15. Frontier orbital interactions for nine-electron (neutral) suprafacial/suprafacial transition structures for [4,5] sigmatropic shifts.

rearranging electrons and a favorable interaction between the LUMO of butadiene and the SOMO of pentadienyl radical would be possible (Fig. 15).

Stationary points and IRC plots for nine-electron [4,5] shifts in the parent system and systems with tethers of various lengths are shown in Figures 16–20. A trend toward concertedness with reduction in tether length is again observed. The overall barriers for the neutral [4,5] shifts are higher than those for either the cationic or the anionic cases, however. In addition, the lengths of bonds a and b in the neutral intermediates are shorter than those in the ionic cases, consistent with previous observations that conjugated radical π-systems tend to be less delocalized than conjugated ionic π-systems;[16] this behavior carries over to hyperconjugation here. In contrast to the ionic cases, all of the radical cases examined begin from minima with intact ring systems.

4. Relationship to (5+4) cycloadditions

As described above, while looking for [4,5] sigmatropic shift reactions, we found some pathways that appear to involve (5+4) cycloadditions.[17] [4,5] Sigmatropic shifts and (5+4) cycloadditions are fundamentally connected in that both involve the interaction between pentadienyl and butadiene substructures, and predicting whether either of such reactions is orbital symmetry allowed involves analysis of the frontier orbitals of these structural units.[6]

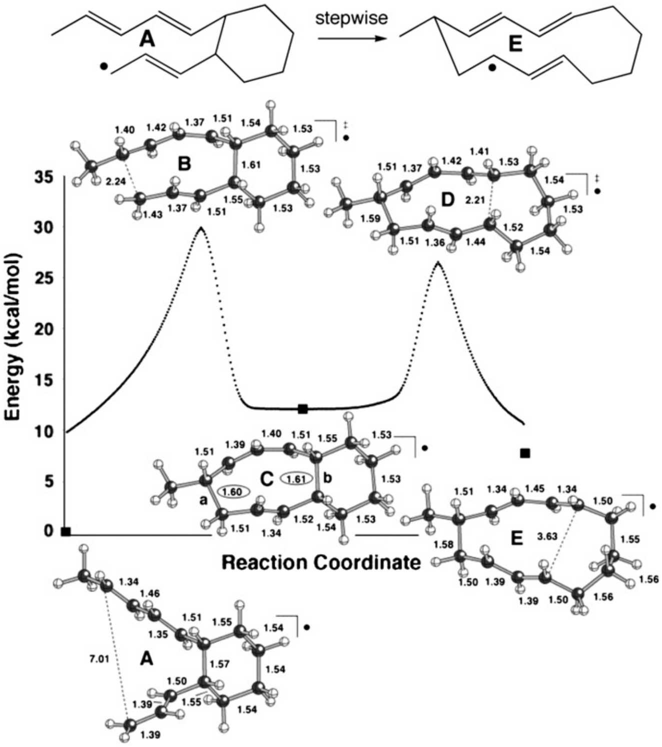

Figure 17. Computed (UB3LYP/6-31G(d)) structures involved in the neutral [4,5] shift for the system with a four-methylene tether. Selected distances are shown in angstroms.

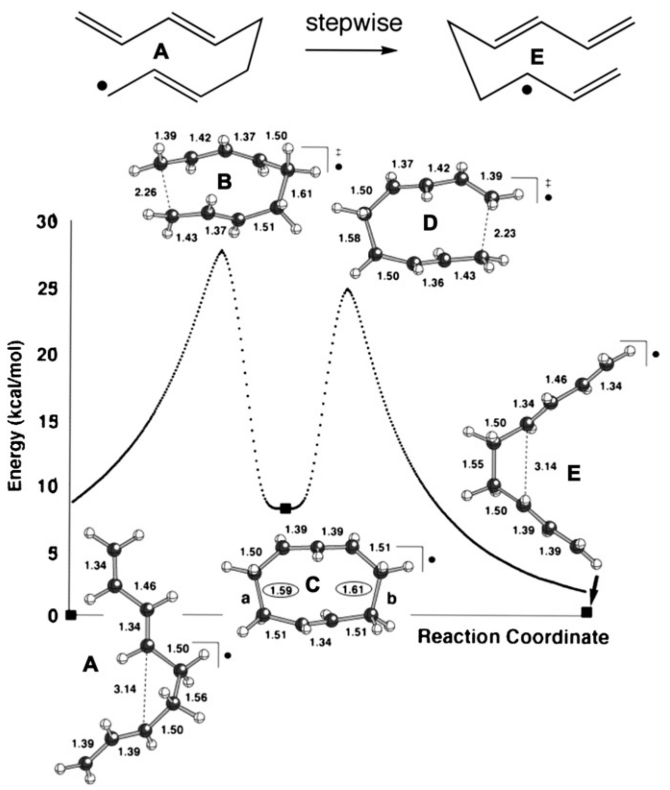

Figure 16. Computed (UB3LYP/6-31G(d)) structures involved in the neutral [4,5] shift for the parent system. Selected distances are shown in angstroms.

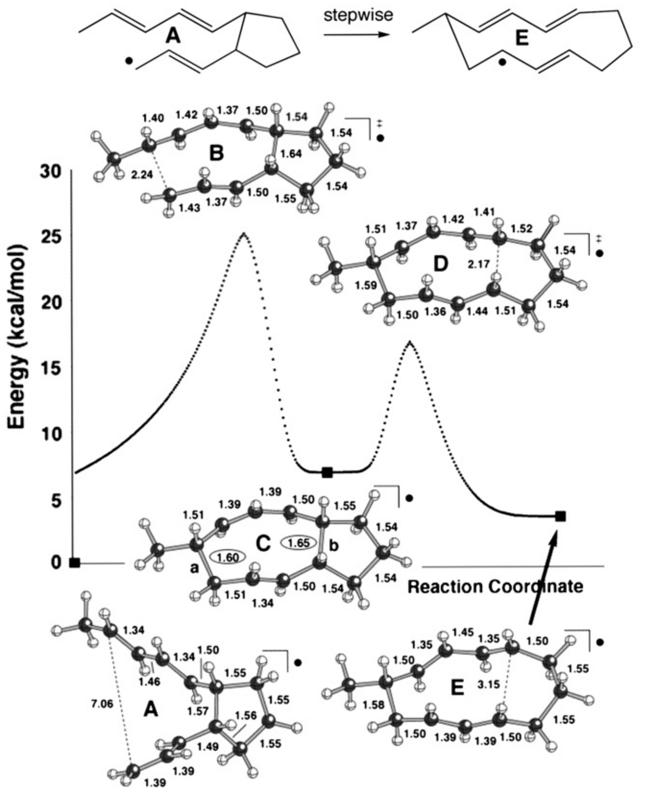

Figure 18. Computed (UB3LYP/6-31G(d)) structures involved in the neutral [4,5] shift for the system with a three-methylene tether. Selected distances are shown in angstroms.

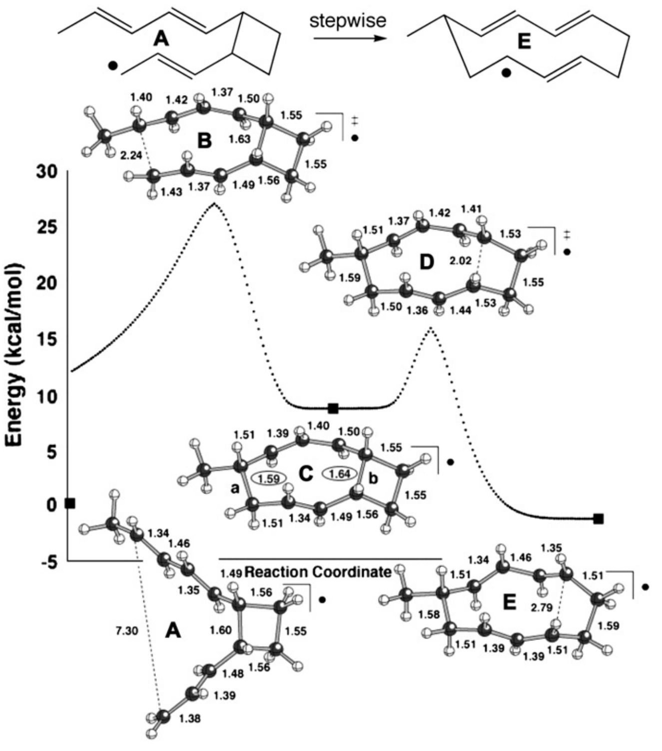

Figure 19. Computed (UB3LYP/6-31G(d)) structures involved in the neutral [4,5] shift for the system with a two-methylene tether. Selected distances are shown in angstroms.

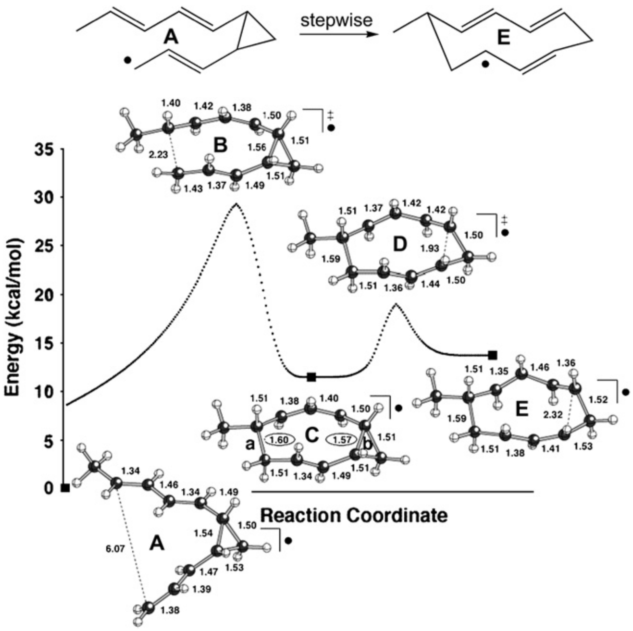

Figure 20. Computed (UB3LYP/6-31G(d)) structures involved in the neutral [4,5] shift for the system with a one-methylene tether. Selected distances are shown in angstroms.

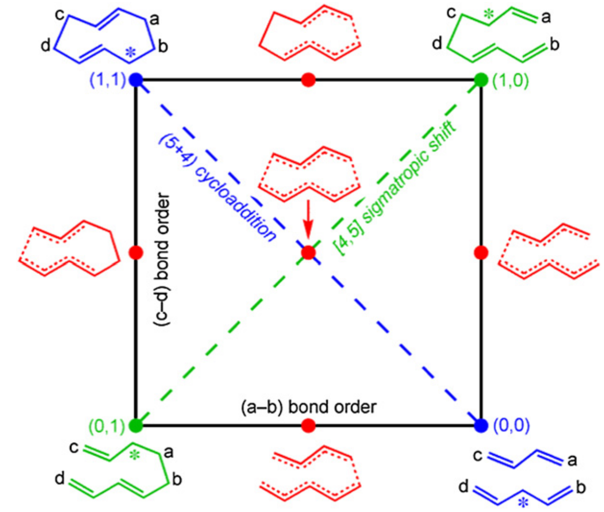

Figure 21. More O'Ferrall–Jencks-style diagram highlighting the relationship between [4,5] sigmatropic shifts and (5+4) cycloadditions. The horizontal axis corresponds to the bond order of the a–b bond, while the vertical axis corresponds to the bond order of the c–d bond. The minima involved in the [4,5] sigmatropic shift are shown in green and the minima involved in the (5+4) cycloaddition are shown in blue. All transition state structures are shown in red and are assumed here, for the sake of discussion, to have partial single bonds of order 0.5. Note that with this assumption, the transition state structures for the concerted [4,5] sigmatropic shift and the (5+4) cycloaddition are the same.

The connection between these two types of reaction is perhaps best explained using a More O'Ferrall–Jencks-style diagram (Fig. 21).[18] The reactant for our parent [4,5] shift is shown in green at the bottom left of Figure 21 (bond orders of (0,1)). A concerted, synchronous [4,5] sigmatropic shift of this structure would correspond to the dotted green line that connects it to the top right green structure with bond orders (1,0). Alternatively, this [4,5] sigmatropic shift could occur in stepwise fashion, which would correspond to moving along the edges of the plot in one of two ways. Either the bottom left structure would be transformed into the top left blue structure with bond orders (1,1) and then to the top right structure with bond orders (1,0), or it could be first transformed into the bottom right blue structure with bond orders (0,0) before being converted to the top right structure. The concerted (4,5) shifts described above involve pathways that first move toward the top left structure but do not actually reach it before turning toward the top right structure.

Interestingly, the bottom right blue structure with bond orders (0,0) could do a concerted, synchronous (5+4) cycloaddition to get to the top left blue structure with bond orders (1,1). Note that based on this simplified analysis, the transition state structures for the concerted and synchronous [4,5] shifts and the concerted and synchronous (5+4) cycloadditions are expected to be the same! Such a situation has been described previously in the context of the so-called 'bis-pericyclic' reactions.[19] For the systems described herein, however, no concerted and synchronous pathways of any sort were located. The reactions shown in Figures 13 and 14 can be described as processes that start at the bottom right structure then move near to (but not all the way to) the bottom left structure, then to the top left structure, and then horizontally to the top right structure.[20]

5. Summary

Herein, we have described a collection of rearrangements that are formally, but not truly, pericyclic. Although some of these processes are concerted, the bond making and breaking events involved occur quite asynchronously,[7] thereby avoiding the unfavorable orbital interactions that, in some cases, would make these processes 'forbidden'. Some of these processes may be relevant to the biosynthesis of ladderane lipids, but this awaits experimental testing. In general, we hope that the computational results described herein will provide new jumping off points for experimentalists interested in ionic rearrangements and the limits of pericyclic behavior.

Acknowledgements

We gratefully acknowledge the University of California, Davis, the donors of the American Chemical Society Petroleum Research Fund, the National Science Foundation CAREER program, and the National Science Foundation's Partnership for Advanced Computational Infrastructure (Pittsburgh Supercomputer Center) for support.

Supplementary data

Coordinates and energies for all structures along with additional results and discussion on small model systems can be found in the online version. Supplementary data associated with this article can be found in the online version, at doi:10.1016/j.tet.2008.04.028.

References and notes

1. (a) Nouri, D. H.; Tantillo, D. J. *Curr. Org. Chem.* **2006**, *10*, 2055–2074; (b) Hopf, H. *Angew. Chem., Int. Ed.* **2003**, *42*, 2822–2825.
2. For representative examples on synthetic approaches to ladderanes, see: (a) Mehta, G.; Viswanath, M. B.; Kunwar, A. C. *J. Org. Chem.* **1994**, *59*, 6131–6132; (b) Martin, H.-D.; Mayer, B.; Pütter, M.; Höchstetter, H. *Angew. Chem., Int. Ed. Engl.* **1981**, *20*, 677–678; (c) Mascitti, V.; Corey, E. J. *J. Am. Chem. Soc.* **2006**, *128*, 3118–3119; (d) Gao, X.; Friščić, T.; MacGillivray, L. R. *Angew. Chem., Int. Ed.* **2004**, *43*, 232–236.
3. (a) Damsté, J. S. S.; Strous, M.; Rijpstra, W. I. C.; Hopmans, E. C.; Geenevasen, J. A. J.; van Duin, A. C. T.; van Niftrik, L. A.; Jetten, M. S. M. *Nature* **2002**, *419*, 708–712; (b) Kuypers, M. M. M.; Sliekers, A. O.; Lavik, G.; Schmid, M.; Jørgensen, B. B.; Kuenen, J. G.; Damsté, J. S. S.; Strous, M.; Jetten, M. S. M. *Nature* **2003**, *422*, 608–611.
4. Nouri, D. H.; Tantillo, D. J. *J. Org. Chem.* **2006**, *71*, 3686–3695.
5. Nouri, D. H. A theoretical mechanistic study of [3]- and [5]-ladderane lipids, and the origin of the hiscotropic rearrangement. Ph.D. Thesis, University of California—Davis: Davis, CA, December 2007.
6. (a) Woodward, R. B.; Hoffmann, R. *The Conservation of Orbital Symmetry*; Chemie: Weinheim, Germany, 1970; (b) Hoffmann, R.; Woodward, R. B. *Acc. Chem. Res.* **1968**, *1*, 17–22; (c) Woodward, R. B.; Hoffmann, R. *Angew. Chem., Int. Ed. Engl.* **1969**, *8*, 781–853.
7. Tantillo, D. J. *J. Phys. Org. Chem.*, in press.
8. Houk, K. N.; Li, Y.; Evanseck, J. D. *Angew. Chem., Int. Ed. Engl.* **1992**, *31*, 682–708.
9. Frisch, M. J.; Trucks, G. W.; Schlegel, H. B.; Scuseria, G. E.; Robb, M. A.; Cheeseman, J. R.; Montgomery, J. A., Jr.; Vreven, T.; Kudin, K. N.; Burant, J. C.; Millam, J. M.; Iyengar, S. S.; Tomasi, J.; Barone, V.; Mennucci, B.; Cossi, M.; Scalmani, G.; Rega, N.; Petersson, G. A.; Nakatsuji, H.; Hada, M.; Ehara, M.; Toyota, K.; Fukuda, R.; Hasegawa, J.; Ishida, M.; Nakajima, T.; Honda, Y.; Kitao, O.; Nakai, H.; Klene, M.; Li, X.; Knox, J. E.; Hratchian, H. P.; Cross, J. B.; Adamo, C.; Jaramillo, J.; Gomperts, R.; Stratmann, R. E.; Yazyev, O.; Austin, A. J.; Cammi, R.; Pomelli, C.; Ochterski, J. W.; Ayala, P. Y.; Morokuma, K.; Voth, G. A.; Salvador, P.; Dannenberg, J. J.; Zakrzewski, V. G.; Dapprich, S.; Daniels, A. D.; Strain, M. C.; Farkas, O.; Malick, D. K.; Rabuck, A. D.; Raghavachari, K.; Foresman, J. B.; Ortiz, J. V.; Cui, Q.; Baboul, A. G.; Clifford, S.; Cioslowski, J.; Stefanov, B. B.; Liu, G.; Liashenko, A.; Piskorz, P.; Komaromi, I.; Martin, R. L.; Fox, D. J.; Keith, T.; Al-Laham, M. A.; Peng, C. Y.; Nanayakkara, A.; Challacombe, M.; Gill, P. M. W.; Johnson, B.; Chen, W.; Wong, M. W.; Gonzalez, C.; Pople, J. A. *GAUSSIAN03, revision B.04*; Gaussian: Pittsburgh, PA, 2003.
10. (a) Becke, A. D. *J. Chem. Phys.* **1993**, *98*, 5648–5652; (b) Becke, A. D. *J. Chem. Phys.* **1993**, *98*, 1372–1377; (c) Lee, C.; Yang, W.; Parr, R. G. *Phys. Rev. B* **1988**, *37*, 785–789; (d) Stephens, P. J.; Devlin, F. J.; Chabalowski, C. F.; Frisch, M. J. *J. Phys. Chem.* **1994**, *98*, 11623–11627.
11. (a) Gonzalez, C.; Schlegel, H. B. *J. Phys. Chem.* **1990**, *94*, 5523–5527; (b) Fukui, K. *Acc. Chem. Res.* **1981**, *14*, 363–368.
12. Müller, N.; Falk, A. Ball & Stick V.3.7.6, molecular graphics application for MacOS computers.
13. Hoffmann, R. *Acc. Chem. Res.* **1971**, *4*, 1–9.
14. Gutta and Tantillo's 'proton sandwiches' can be described similarly. See: (a) Gutta, P.; Tantillo, D. J. *Angew. Chem., Int. Ed.* **2005**, *44*, 2719–2723; (b) Ponec, R.; Bultinck, P.; Gutta, P.; Tantillo, D. J. *J. Phys. Chem. A* **2006**, *110*, 3785–3789.
15. [4,5] Sigmatropic shifts of ylides involving 10 electrons have been described. See, for example: (a) Laird, T.; Ollis, W. D.; Sutherland, I. O. *J. Chem. Soc., Perkin Trans. 1* **1980**, 2033–2048; (b) Ollis, W. D.; Somanathan, R.; Sutherland, I. O. *J. Chem. Soc., Chem. Commun.* **1973**, 661; (c) Laird, T.; Ollis, W. D. *J. Chem. Soc., Chem. Commun.* **1973**, 658–660.
16. Mo, Y.; Lin, Z.; Wu, W.; Zhang, Q. *J. Phys. Chem.* **1996**, *100*, 6469–6474.
17. For information on a related (4+3) cycloaddition, see: Siebert, M. R.; Tantillo, D. J. *J. Phys. Org. Chem.* **2007**, *20*, 384–394.
18. More O-Ferrall, R. A. *J. Chem. Soc. Sect B: Phys. Org.* **1970**, *2*, 274–277.
19. For examples and leading references, see: (a) Caramella, P.; Quadrelli, P.; Toma, L. *J. Am. Chem. Soc.* **2002**, *124*, 1130–1131; (b) Quadrelli, P.; Romano, S.; Toma, L.; Caramella, P. *Tetrahedron Lett.* **2002**, *43*, 8785–8789; (c) Quadrelli, P.; Romano, S.; Toma, L.; Caramella, P. *J. Org. Chem.* **2003**, *68*, 6035–6038; (d) Leach, A. G.; Goldstein, E.; Houk, K. N. *J. Am. Chem. Soc.* **2003**, *125*, 8330–8339; (e) Limanto, J.; Khuong, K. S.; Houk, K. N.; Snapper, M. L. *J. Am. Chem. Soc.* **2003**, *125*, 16310–16321.
20. Additional results on small model systems can be found in Supplementary data available online.